AIP | The Journal of Chemical Physics

First-principles investigation on the electronic efficiency and binding energy of the contacts formed by graphene and poly-aromatic hydrocarbon anchoring groups

Yang Li, Xingchen Tu, Hao Wang, Stefano Sanvito, and Shimin Hou

Citation: The Journal of Chemical Physics **142**, 164701 (2015); doi: 10.1063/1.4918738
View online: http://dx.doi.org/10.1063/1.4918738
View Table of Contents: http://scitation.aip.org/content/aip/journal/jcp/142/16?ver=pdfcov
Published by the AIP Publishing

First-principles investigation on the electronic efficiency and binding energy of the contacts formed by graphene and poly-aromatic hydrocarbon anchoring groups

Yang Li,[1] Xingchen Tu,[1] Hao Wang,[1] Stefano Sanvito,[2] and Shimin Hou[1,a)]
[1]*Centre for Nanoscale Science and Technology, Key Laboratory for the Physics and Chemistry of Nanodevices, Department of Electronics, Peking University, Beijing 100871, China*
[2]*School of Physics, AMBER and CRANN Institute, Trinity College, Dublin 2, Ireland*

(Received 23 November 2014; accepted 9 April 2015; published online 22 April 2015)

The electronic efficiency and binding energy of contacts formed between graphene electrodes and poly-aromatic hydrocarbon (PAH) anchoring groups have been investigated by the non-equilibrium Green's function formalism combined with density functional theory. Our calculations show that PAH molecules always bind in the interior and at the edge of graphene in the AB stacking manner, and that the binding energy increases following the increase of the number of carbon and hydrogen atoms constituting the PAH molecule. When we move to analyzing the electronic transport properties of molecular junctions with a six-carbon alkyne chain as the central molecule, the electronic efficiency of the graphene-PAH contacts is found to depend on the energy gap between the highest occupied molecular orbital (HOMO) and the lowest unoccupied molecular orbital (LUMO) of the corresponding PAH anchoring group, rather than its size. To be specific, the smaller is the HOMO-LUMO gap of the PAH anchoring group, the higher is the electronic efficiency of the graphene-PAH contact. Although the HOMO-LUMO gap of a PAH molecule depends on its specific configuration, PAH molecules with similar atomic structures show a decreasing trend for their HOMO-LUMO gap as the number of fused benzene rings increases. Therefore, graphene-conjugated molecule-graphene junctions with high-binding and high-conducting graphene-PAH contacts can be realized by choosing appropriate PAH anchor groups with a large area and a small HOMO-LUMO gap. [http://dx.doi.org/10.1063/1.4918738]

I. INTRODUCTION

Since its discovery in 2004,[1] graphene has received enormous attention due to its superior mechanical, optical, electronic, and magnetic properties.[2] Recently graphene has also been employed as electrode material for molecular electronic devices.[3–8] Compared with conventional gold and platinum electrodes, graphene has many advantages. First, its sp^2 covalent C–C bond-structure provides mechanical stability up to temperatures much higher than room temperature. Second, its thickness down to the atomic scale reduces the screening of an applied gate field and thus enhances the gate coupling. More importantly, individual molecules can bind to the graphene electrodes not only through covalent functional groups like amide group but also via π-π stacking interactions of poly-aromatic hydrocarbons (PAHs). In contrast to covalent bonds with a specific bond length and bond angle, π-π stacking interactions are rather fragile. Thus, the requirements for the shape and size of the nanogap between the two graphene electrodes are not too strict.

Although Prins *et al.*, have demonstrated the possibility of fabricating molecular electronic devices at room temperature by depositing molecules with anthracene anchoring groups onto electro-burned few-layer graphene nanogaps,[3] the low-bias conductance measured in their devices is very small. In order to improve the device performance, it is highly desirable to investigate the electronic transport mechanism of such molecular devices, especially the electronic efficiency and thermal stability of the graphene-PAH contacts.[9] Here, we address these issues by employing the non-equilibrium Green's function formalism combined with density functional theory (i.e., the NEGF + DFT approach).[10–19] The electronic transport properties of a molecular device are dominated by the quantum nature of the central molecule, the band structure of the electrodes, and the electronic coupling at the molecule-electrode interfaces. In order to focus on the graphene-PAH contacts, we choose a six-carbon (C_6) alkyne chain with alternating single and triple bonds as the central molecule. Our calculations show that the binding energies of PAH molecules adsorbed in the interior and at the edge of graphene electrodes get larger as the number of carbon and hydrogen atoms contained in the PAH molecule increases. Furthermore, the electronic efficiency of the graphene-PAH contacts is dominated by the energy gap between the highest occupied molecular orbital (HOMO) and the lowest unoccupied molecular orbital (LUMO) of the corresponding PAH anchoring groups. Thus, graphene-PAH contacts with high binding energy and high electronic efficiency can be realized by choosing PAH molecules with a large area and a small HOMO-LUMO gap.

a)Author to whom correspondence should be addressed. Electronic mail: smhou@pku.edu.cn

II. CALCULATION METHOD

Because the π-π stacking interaction is a long-range noncovalent interaction, for geometry optimizations we adopt van der Waals density functional (vdW-DF) implemented in the SIESTA package.[20,21] Although this vdW-DF slightly overestimates covalent bonds,[22] it shows good performances when describing the interlayer distance and the binding energy,[23] both playing a critical role in molecular devices constructed through π-π interactions. In SIESTA, atomic cores are described by improved Troullier–Martins pseudopotentials, and the wave functions of the valence electrons are expanded in terms of a finite-range numerical orbital basis set.[24,25] In this work, a double-zeta plus polarization (DZP) basis set is used for H, C, and N. Geometry optimization is performed by standard conjugate gradient relaxation until the atomic forces are smaller than 0.03 eV $Å^{-1}$. In order to model isolated PAH molecules adsorbed on the two-dimensional graphene sheets, the vacuum layer between the neighboring cells is always larger than 16 Å and the distance between the PAH molecules and their periodic images is larger than 10 Å.

The electronic transport properties of molecular devices incorporating graphene electrodes are calculated using the SMEAGOL package, which is a practical implementation of the NEGF + DFT approach and employs SIESTA as its DFT platform.[17–19] Since it has been shown that the electronic structures obtained with the vdW-DF are essentially the same as those computed with the Perdew–Burke–Ernzerhof (PBE) general gradient approximation (GGA) functional,[26,27] the PBE GGA functional is used for the transport calculations to improve computational efficiency. We use an equivalent cutoff of 200 Ry for the real space grid. The charge density is integrated over 32 energy points along the semi-circle, 32 along the line in the complex plane, while 32 poles are used for the Fermi function (the electronic temperature is 25 meV). Here, the transport is assumed to be along the z-axis and the graphene electrodes are placed in the x-z plane. We always consider periodic boundary condition along the x-axis, so that the graphene electrodes are infinite. The unit cell of the extended molecule comprises the C_6 alkyne chain, two PAH anchoring groups and two graphene electrodes. Each graphene electrode is terminated in a zigzag configuration passivated by hydrogen atoms and has 4–6 principal layers, where each principal layer has 28 carbon atoms in total. The total transmission coefficient $T(E)$ of the junction is evaluated as

$$T(E) = \frac{1}{\Omega_{1DBZ}} \int_{1DBZ} T(\vec{k}, E) d\vec{k}, \quad (1)$$

where Ω_{1DBZ} is the length of the one-dimensional Brillouin zone (1DBZ) along the x-axis. The k-dependent transmission coefficient $T(\vec{k}; E)$ is obtained as

$$T(\vec{k}, E) = Tr[\Gamma_L G_M^R \Gamma_R G_M^{R+}], \quad (2)$$

where G_M^R is the retarded Green's function matrix of the extended molecule and Γ_L (Γ_R) is the broadening function matrix describing the interaction of the extended molecule with the left-hand (right-hand) side electrode. Here, we calculate the transmission coefficient by sampling 4 k-points in the transverse 1DBZ.

III. RESULTS AND DISCUSSION

A. Linear polyacenes as the anchoring group

The strength of the π-π interaction between a planar PAH anchoring group and the graphene electrode is the prerequisite to fabricating stable molecular devices. We first investigate the adsorption geometry and the binding energy of several typical PAH molecules on the graphene electrode. The simplest PAHs are polyacenes made up of linearly fused benzene rings. We choose benzene, naphthalene, anthracene, tetracene, and pentacene as the representatives of polyacenes. When these polyacenes adsorb on the surface of an infinite graphene layer, the AB stacking is always the most stable structure. This is consistent with previous results.[28–30] The binding energies (E_{bind}) computed by taking into account basis set superposition error (BSSE) corrections are, respectively, 0.45 eV (benzene), 0.73 eV (naphthalene), 0.98 eV (anthracene), 1.23 eV (tetracene), and 1.48 eV (pentacene), thus forming approximately an arithmetic progression with common difference of 0.25 eV. This is verified by the binding energy of an infinite one-dimensional polyacene adsorbed on graphene, which is determined to be 0.25 eV per unit cell. Thus, the binding energies of polyacenes on the graphene surface increase linearly following the increase of the number of fused benzene rings. This is further illustrated by plotting the binding energies per carbon atom as a function of the ratio of hydrogen to carbon in these polyacenes (Fig. 1). The blue line shows a fit to the formula $E_{bind} = N_C E_{CC} + N_H(E_{CH} - E_{CC})$ with parameters E_{CC} = 51.8 meV and E_{CH} = 76.4 meV, in which N_C and N_H are, respectively, the number of carbon atoms and the number of hydrogen atoms in each polyacene molecule.[28] The obtained values of the two parameters E_{CC} and E_{CH}, which are, respectively, the fitted energy per graphene-like carbon and that per benzene-like carbon and its associated hydrogen atom, are in good agreement with the values of 49.2 meV and 80.1 meV reported in Ref. 28. The small difference may originate from the fact that in our simulations, the molecules are allowed to distort whereas the molecules are constrained to remain planar in Ref. 28. Furthermore, the distances between the molecular plane and the graphene

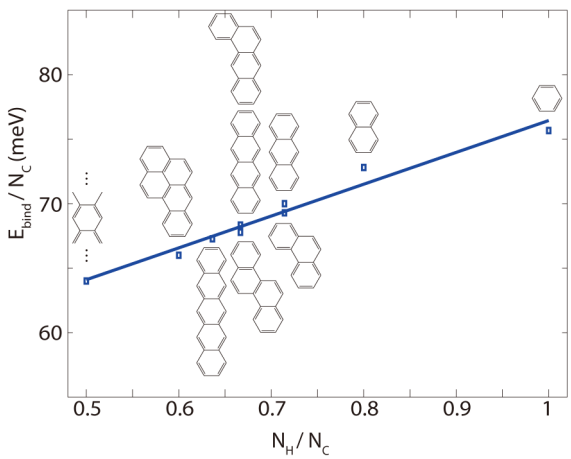

FIG. 1. Binding energy per carbon atom for PAH molecules adsorbed on graphene with the AB stacking configuration; molecular structures of the linear and angular PAH molecules investigated here are also given.

surface are optimized to be in a narrow range between 3.41 Å and 3.44 Å except for benzene (3.32 Å).

In real molecular devices, the anchoring groups may bind at the edge of the graphene electrodes. So it is important to know the difference between the adsorption energy of polyacenes in the interior of graphene and that at an edge. For simplicity, here we only investigate the adsorption of benzene, naphthalene, and anthracene at the defect-free zigzag edge of graphene, where the dangling bonds are passivated with hydrogen atoms. The AB stacking is still the most stable binding configuration, and the binding energies are, respectively, 0.41 eV (benzene), 0.63 eV (naphthalene), and 0.85 eV (anthracene), slightly smaller than the corresponding values calculated for the adsorption in the interior of graphene.

Then, we investigate the electronic transport properties of molecular devices using graphene-polyacene contacts. Fig. 2(a) shows a junction model in which two anthracene molecules are used to attach the C_6 alkyne chain to two semi-infinite graphene electrodes with H-passivated zigzag edges. The equilibrium transmission spectra for devices using benzene, naphthalene, and anthracene anchoring groups are, respectively, given in Figures 2(b)–2(d). As we can see, the transmission coefficients around the Fermi level, E_F, are always very small, though some transmission peaks approaching unity appear far from the Fermi level. Correspondingly, the electric current at low bias is very small. By observing the zoom-in insets in Figures 2(b)–2(d), we can find that the low-transmission region around E_F becomes narrower as the number of fused benzene rings in the anchoring groups increases.

A deeper understanding can be obtained by projecting the density of states (DOS) and the transmission onto the frontier molecular orbitals of the entire molecule including the two anchoring groups and the C_6 alkyne chain.[31] Taking anthracene as an example (Fig. 3), the first transmission peaks below and above the Fermi level are dominated by the HOMO and LUMO of the entire molecule, respectively. As shown in the isosurfaces of Fig. 3(c), the HOMO (LUMO) of the entire molecule is formed by the HOMO (LUMO) of the two anchoring groups and the $2p_y$ orbitals of the carbon atoms in the alkyne chain. When the anchoring groups change from benzene through naphthalene to anthracene, the HOMO-dominated peak shifts upward and the LUMO-dominated one shifts downward in energy. Thus, in order to investigate the limits of the positions of the HOMO- and LUMO-dominated transmission peaks, we construct a junction model with two infinite one-dimensional polyacenes as the anchoring groups. In this case, the two transmission peaks closest to the Fermi level are shifted to −0.27 eV and 0.23 eV, respectively. However, the transmission between these two peaks remains very small though the DOS of the infinite one-dimensional polyacene is continuous around the Fermi level (Fig. S1 in the supplementary material).[32] Since alkyne chains have a high conductance[33–37] and considering that perfect graphene is a zero-gap semiconductor, the low transmission near the Fermi

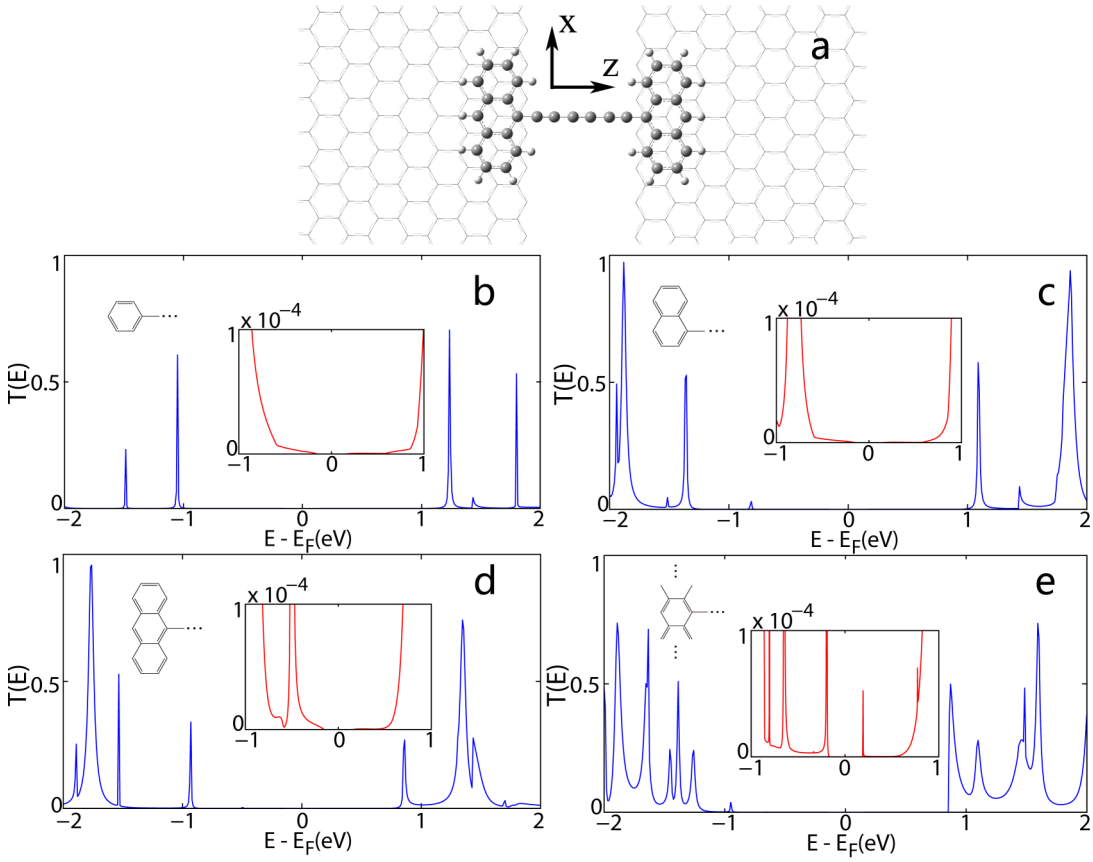

FIG. 2. Schematic diagram (a) of the atomic structure of the junction with one C_6 alkyne chain connected to two semi-infinite graphene electrodes through two anthracene anchoring groups; the equilibrium transmission spectra of symmetric molecular junctions with one C_6 alkyne chain connected to two graphene electrodes through benzene (b), naphthalene (c), anthracene (d), and infinite polyacene (e). The insets show the zoom-in transmission spectra around the Fermi level and the connecting site of the C_6 alkyne chain to the polyacene molecules.

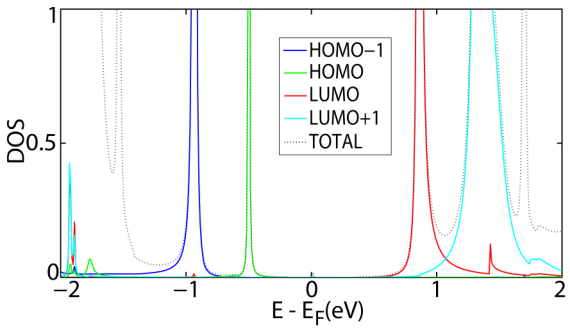

(a)

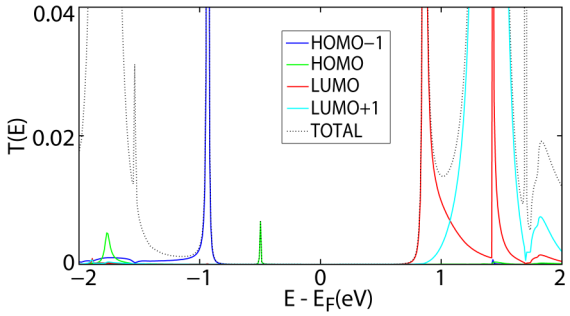

(b)

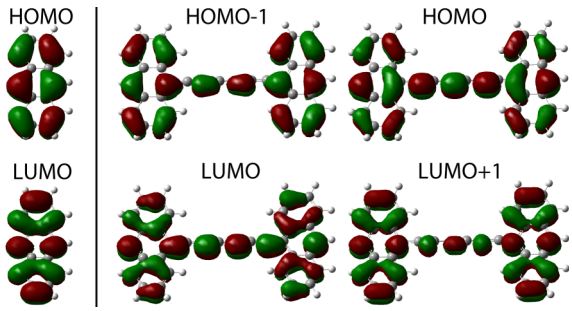

(c)

FIG. 3. DOS (a) and transmission spectrum (b) of the junction with one C_6 alkyne chain connected to graphene electrodes through two anthracene anchoring groups projected onto frontier molecular orbitals of the entire molecule. Frontier molecular orbitals (c) of the entire molecule including the C_6 alkyne chain and two anthracene molecules.

level must originate from the band structure of the graphene electrodes and/or the electronic coupling at the graphene-polyacene contacts.

In order to distinguish the role played by the graphene electrode and the graphene-polyacene contacts, we replace perfect graphene with N-doped graphene, since defects and dopants shift the graphene Fermi level, thus increasing the DOS. It has been proved that graphene with substitutional nitrogen dopants is an n-type conductor.[38] When the dopant concentration is chosen to be 1/28 (one C atom over 28 is replaced by N), the N-doped graphene has a finite DOS around E_F and the Dirac point is shifted down to −0.84 eV (Fig. S2 in the supplementary material).[32] We have calculated the low-bias conductance of the C_6 alkyne chain connected directly to two semi-infinite N-doped graphene electrodes and found that the transmission coefficient at E_F reaches 0.6, while the low transmission region moves to about −0.8 eV (Fig. S3 in the supplementary material).[32] Therefore, N-doped graphene can provide enough conducting channels around the Fermi level, and the graphene-polyacene contacts will dominate the electronic transport properties of molecular junctions in which the C_6 alkyne chain is connected to N-doped graphene electrodes through polyacene anchoring groups.

Nitrogen dopants affect only slightly the adsorption of polyacenes in the interior or at the edge of graphene. Taking anthracene as an example, both the inter-planar distance and the binding energy are very close to those calculated for clean graphene, at least as long as the bonding sites are far away from a nitrogen atom. Even when the anthracene molecule is directly above a nitrogen atom, the inter-planar distance is only decreased by 0.03 Å and the binding energy is increased by 0.03 eV. Fig. 4(a) presents the device model for N-doped graphene electrodes, in which the two anthracene groups are located far away from the nitrogen dopants in order to minimize their effects on the binding configuration. The equilibrium transmission spectra with naphthalene, anthracene, pentacene, and an infinite polyacene as the anchoring groups are, respectively, given in Figures 4(b)–4(e). As the number of fused benzene rings increases, the transmission coefficient around the Fermi level increases substantially; for pentacene, $T(E_F)$ reaches 10^{-3}. This is comparable to the measured low-bias conductances of $(8.1 \pm 0.9) \times 10^{-4}$ G_0 for the C_4 alkyne chain and of $(2.0 \pm 0.6) \times 10^{-4}$ G_0 for C_8 connected to two gold electrodes through the anchor dihydrobenzo[b]thiophene.[39] When two infinite one-dimensional polyacenes are used as the anchoring groups, the transmission coefficient calculated at 0.02 eV above E_F is 0.3, illustrating that high electronic transfer efficiency can be achieved for the graphene-polyacene contacts when the polyacene anchoring group is long enough. It should be noted that in these junction models, the polyacene anchoring groups are assumed to bind above the zigzag edges of the graphene electrodes and thus the edge state and spin polarization at the zigzag edge will affect the junction transport properties.[40,41] For example, the transmission peaks appearing at about −57 meV below the Fermi level shown in Figures 4(b)–4(d) are mainly contributed by the edge state at the zigzag edge. This can be seen clearly from the local density of states (LDOS) of the carbon atoms at the zigzag edge (see Fig. S4 in the supplementary material).[32] Spin polarization also modifies the junction transmission spectrum slightly (see Fig. S5 in the supplementary material).[32] However, in practice, it is extremely difficult to control the atomic structures of graphene edges in experiments,[42] and both armchair and chiral edges with chiral angle larger than a critical value do not show spin polarization.[43] Furthermore, the effects arising from the graphene edge on the junction transmission reduce when the polyacenes bind to the graphene electrodes away from their edges. Therefore, we have not investigated the effects of the zigzag edges in more details.

B. Angular PAHs as the anchoring group

Although increasing the number of fused benzene rings in the polyacene anchoring group can enhance the electronic efficiency at the graphene-polyacene contact, polyacenes longer than pentacene become unstable in air.[44] Therefore, we investigate the effects of the detailed molecular configuration on the transport properties of graphene-PAH contacts. Here,

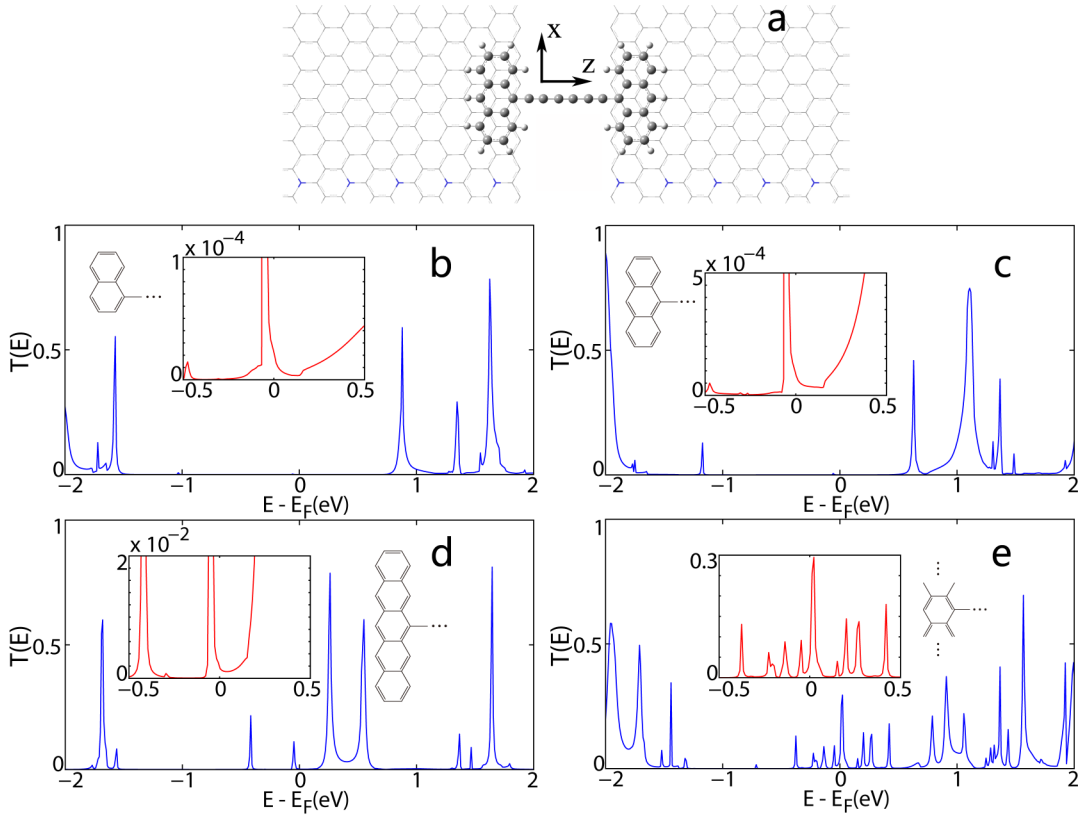

FIG. 4. Schematic diagram (a) of the atomic structure of a junction comprising one C_6 alkyne chain connected to two N-doped graphene electrodes through two anthracene anchoring groups, the blue dots represent nitrogen dopants; the equilibrium transmission spectra of symmetric molecular junctions constructed with one C_6 alkyne chain connected to N-doped graphene electrodes through naphthalene (b), anthracene (c), pentacene (d), and infinite polyacene (e). The insets show the zoom-in transmission spectra around the Fermi level and the connecting site of the C_6 alkyne chain to the polyacene molecules.

we choose phenanthrene, chrysene, benz[a]anthrene, and benzo[a]pyrene as prototypes in which the benzene rings are fused so to produce angular molecules, in contrast to polyacenes, where benzene rings are fused in a linear way. When these four angular PAH molecules adsorb on the graphene surface in a AB stacking manner, the average inter-planar distances are between 3.41 Å and 3.42 Å. The binding energies obtained by including BSSE corrections are, respectively, 0.97 eV (phenanthrene), 1.22 eV (chrysene), 1.23 eV (benz[a]anthrene), and 1.32 eV (benzo[a]pyrene), i.e., they do increase monotonically as the molecule gets larger. When comparing with linear polyacenes, we find that the molecular configuration has only a minor influence on the binding energies of linear and angular PAH molecules. For example, chrysene, benz[a]anthrene, and tetracene are isomers, and the difference of their calculated binding energies is less than 0.01 eV. Similarly to the cases of polyacenes, nitrogen dopants only affect slightly the adsorption properties of angular PAH molecules in the interior or at the edge of graphene. Therefore, as the number of carbon and hydrogen atoms in PAHs increases, the binding energies in the AB stacking manner always increase while the inter-planar distance remains constant. In conclusion, as long as a PAH anchoring group is large enough, it can form a high-binding contact with graphene.

Now we investigate the electronic transport properties of the C_6 alkyne chain connected to N-doped graphene through angular PAH anchoring groups. As it can be seen from the calculated equilibrium transmission spectra (Figures 5(b)–5(e)), both the positions of the transmission peaks closest to the Fermi level and the transmission coefficients around the Fermi level do not have a simple relation with the number of fused benzene rings. For example, benz[a]anthrene and chrysene are isomers, but the transmission coefficient of the junction at E_F for the benz[a]anthrene anchoring groups is larger than that with the chrysene ones. When comparing with the cases of polyacenes, the low-bias conductance of the junction with the benz[a]anthrene anchoring groups is much closer to that of anthracene groups than that with the tetracene ones, although benz[a]anthrene and tetracene are isomers. This indicates that, different from the binding energies, the electronic efficiency of the graphene-PAH contacts is not determined by the size of the PAH anchoring groups.

Similarly to the case of polyacene, around the Fermi level the transmission of the junctions constructed with angular PAH anchoring groups is also dominated by the HOMO and LUMO of the entire molecule. Because the HOMO (LUMO) of the entire molecule is formed by the HOMO (LUMO) of the two anchoring groups and the $2p_y$ atomic orbitals of the alkyne chain and it is thus delocalized along the entire molecule, we calculate the HOMO-LUMO gap of these linear and angular PAH molecules. As listed in Table I, the HOMO-LUMO gap of polyacenes decreases monotonically as the number of fused benzene rings increases. In contrast, the dependence of the HOMO-LUMO gap of angular PAH molecules on their constitution and configuration is more complex. Although the general trend that the HOMO-LUMO gap decreases as

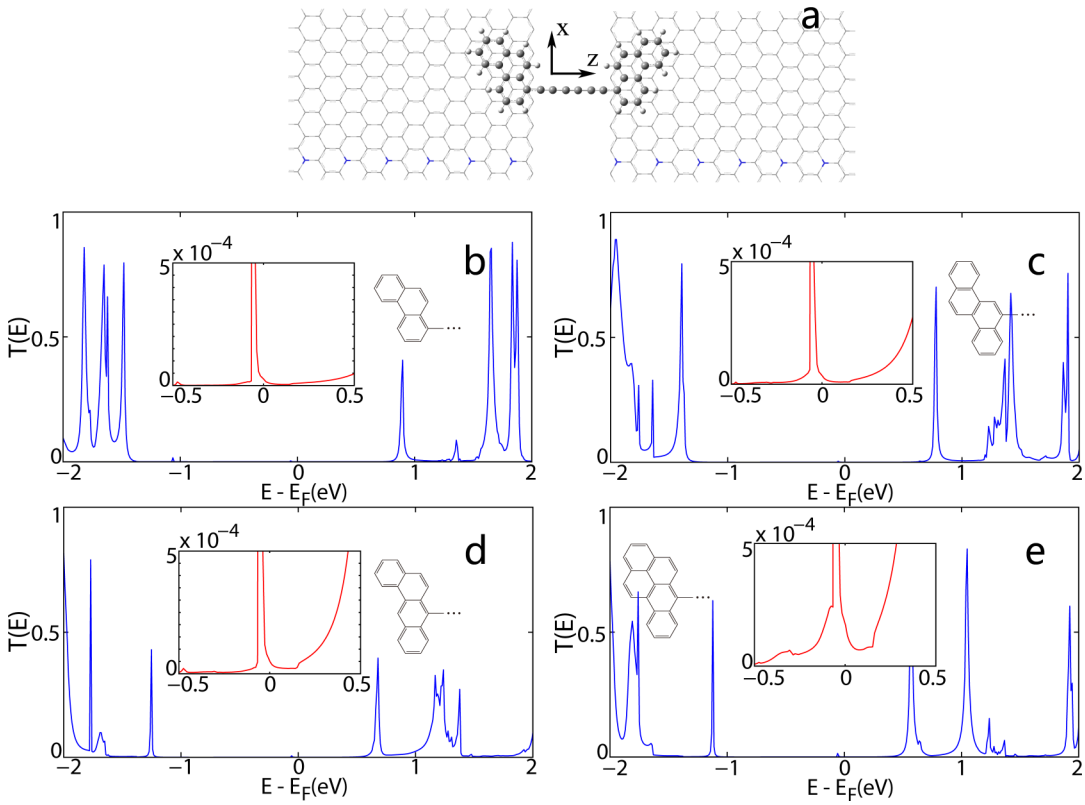

FIG. 5. Schematic diagram (a) of the atomic structure of a junction comprising one C_6 alkyne chain connected to two N-doped graphene electrodes through two phenanthrene anchoring groups, the blue dots represent nitrogen dopants; the equilibrium transmission spectra of symmetric molecular junctions with one C_6 alkyne chain connected to N-doped graphene electrodes through phenanthrene (b), chrysene (c), benz[a]anthrene, (d) and benzo[a]pyrene (e). The insets show the zoom-in transmission spectra around the Fermi level and the connecting site of the C_6 alkyne chain to the angular PAH molecules.

the conjugation increases is still correct for angular PAH molecules with similar atomic structure, the HOMO-LUMO gap of angular PAH molecules with different atomic structures depends on their specific configuration. If we compare the equilibrium transmission spectra shown in Figs. 4 and 5, we will find that the low-bias conductance of the junction is directly related to the HOMO-LUMO gap of the corresponding PAH anchoring groups: the smaller is the HOMO-LUMO gap, the larger is $T(E_F)$, and the higher is the electronic efficiency of the graphene-PAH contacts. As a result, among the linear and angular PAH molecules investigated here pentacene is the best candidate for connecting the targeted molecule to the two graphene electrodes due to its large binding energy (1.48 eV) and small HOMO-LUMO gap (1.11 eV). If one wants to further improve the binding energy and electronic efficiency of the graphene-PAH contacts, other angular PAH molecules with a larger size and a smaller HOMO-LUMO gap than those of pentacene should be selected.

TABLE I. The HOMO-LUMO gap of linear and angular PAH molecules calculated using the PBE GGA functional.

Linear PAH molecules	HOMO-LUMO gap (eV)	Angular PAH molecules	HOMO-LUMO gap (eV)
Benzene	4.88	Phenanthrene	3.21
Naphthalene	3.24	Chrysene	2.81
Anthracene	2.22	Benz[a]anthracene	2.39
Tetracene	1.57	Benzo[a]pyrene	2.11
Pentacene	1.11		

IV. CONCLUSION

We have investigated the electronic transfer efficiency and the binding energy of graphene-PAH contacts using the NEGF + DFT approach, and found that AB stacking is always the most stable binding geometry for both linear and angular PAH molecules and that the binding energy increases monotonically following the increase of the number of carbon and hydrogen atoms in PAHs. The overall binding energies of PAH molecules larger than anthracene are more than 1.0 eV and thus they can be used to connect the selected central molecule to the graphene electrodes forming molecular junctions. As demonstrated by our electronic transport calculations for symmetric graphene-PAH-C_6-PAH-graphene molecular junctions, the electronic efficiency of the graphene-PAH contacts is directly related to the HOMO-LUMO gap of the PAH anchoring groups. PAH anchoring groups with smaller HOMO-LUMO gap result in graphene-PAH contacts with higher electronic efficiency. Furthermore, the HOMO-LUMO gap of linear polyacenes decreases as the number of fused benzene rings increases. Although the HOMO-LUMO gap of angular PAHs depends on their specific configurations, PAH molecules with similar atomic structures do show a decreasing trend in their HOMO-LUMO gap following the

increase of the number of fused benzene rings. Therefore, graphene-molecule-graphene junctions with high-binding and high-conducting graphene-PAH contacts can be constructed by choosing appropriate PAH anchoring groups with a large area and a small HOMO-LUMO gap. These findings will help the design of molecular devices with graphene electrodes. It should be noted that the energy barrier for these PAH molecules to displace from the AB stacking configuration is comparable with the thermal energy K_BT at room temperature (0.025 eV). Thus, these PAH molecules are mobile over the graphene surface at room temperature.[45] PAH-graphene contacts with high thermal stability may be fabricated by attaching suitable side groups onto the PAH molecules, an aspect requiring further investigations in the future.

ACKNOWLEDGMENTS

This project was supported by the National Natural Science Foundation of China (No. 61321001) and the MOST of China (Nos. 2011CB933001 and 2013CB933404). S.S. thanks additional funding support from the European Research Council (QUEST project), by KAUST (FIC/2010/08), and by AMBER (12/RC/2278).

[1]K. S. Novoselov, A. K. Geim, S. V. Morozov, D. Jiang, Y. Zhang, S. V. Dubonos, I. V. Grigorieva, and A. A. Firsov, Science **306**, 666 (2004).
[2]K. S. Novoselov, V. I. Fal'ko, L. Colombo, P. R. Gellert, M. G. Schwab, and K. Kim, Nature **490**, 192 (2012).
[3]F. Prins, A. Barreir, J. W. Ruitenberg, J. S. Seldenthuis, N. Aliaga-Alcalde, L. M. K. Vandersypen, and H. S. J. van der zant, Nano Lett. **11**, 4607 (2011).
[4]Y. Cao, S. Dong, S. Liu, L. He, L. Gan, X. Yu, M. L. Steigerwald, X. Wu, Z. Liu, and X. Guo, Angew. Chem., Int. Ed. **51**, 12228 (2012).
[5]Y. Cao, S. Dong, S. Liu, Z. Liu, and X. Guo, Angew. Chem., Int. Ed. **52**, 3906 (2013).
[6]C. Jia, J. Wang, C. Yao, Y. Cao, Y. Zhong, Z. Liu, Z. Liu, and X. Guo, Angew. Chem., Int. Ed. **52**, 8666 (2013).
[7]C. G. Péterfalvi and C. J. Lambert, Phys. Rev. B **86**, 085443 (2012).
[8]V. M. García-Suárez, R. Ferradás, D. Carrascal, and J. Ferrer, Phys. Rev. B **87**, 235425 (2013).
[9]E. Lörtscher, Nat. Nanotechnol. **8**, 381 (2013).
[10]Y. Meir and N. S. Wingreen, Phys. Rev. Lett. **68**, 2512 (1992).
[11]P. Hohenberg and W. Kohn, Phys. Rev. **136**, B864 (1964).
[12]W. Kohn and L. J. Sham, Phys. Rev. **140**, A1133 (1965).
[13]Y. Xue, S. Datta, and M. A. Ratner, Chem. Phys. **281**, 151 (2002).
[14]M. Brandbyge, J.-L. Mozos, P. Ordejón, J. Taylor, and K. Stokbro, Phys. Rev. B **65**, 165401 (2002).
[15]J. Zhang, S. Hou, R. Li, Z. Qian, R. Han, Z. Shen, X. Zhao, and Z. Xue, Nanotechnology **16**, 3057 (2005).
[16]R. Li, J. Zhang, S. Hou, Z. Qian, Z. Shen, X. Zhao, and Z. Xue, Chem. Phys. **336**, 127 (2007).
[17]A. R. Rocha, V. M. Garcia-Suarez, S. W. Bailey, C. J. Lambert, J. Ferrer, and S. Sanvito, Nat. Mater **4**, 335 (2005).
[18]A. R. Rocha, V. M. García-Suárez, S. Bailey, C. Lambert, J. Ferrer, and S. Sanvito, Phys. Rev. B **73**, 085414 (2006).
[19]I. Rungger and S. Sanvito, Phys. Rev. B **78**, 035407 (2008).
[20]M. Dion, H. Rydberg, E. Schröder, D. C. Langreth, and B. I. Lundqvist, Phys. Rev. Lett. **92**, 246401 (2004).
[21]G. Román-Pérez and J. M. Soler, Phys. Rev. Lett. **103**, 096102 (2009).
[22]J. Klimeš, D. R. Bowler, and A. Michaelides, Phys. Rev. B **83**, 195131 (2011).
[23]S. D. Chakarova-Käck, E. Schröder, B. I. Lundqvist, and D. C. Langreth, Phys. Rev. Lett. **96**, 146107 (2006).
[24]N. Troullier and J. Martins, Phys. Rev. B **43**, 1993 (1991).
[25]J. M. Soler, E. Artacho, J. D. Gale, A. García, J. Junquera, P. Ordejón, and D. Sánchez-Portal, J. Phys.: Condens. Matter **14**, 2745 (2002).
[26]I. Hamada and S. Yanagisawa, Phys. Rev. B **84**, 153104 (2011).
[27]J. Perdew, K. Burke, and M. Ernzerhof, Phys. Rev. Lett. **77**, 3865 (1996).
[28]J. Björk, F. Hanke, C.-A. Palma, P. Samori, M. Cecchini, and M. Persson, J. Phys. Chem. Lett. **1**, 3407 (2010).
[29]S. D. Chakarova-Käck, A. Vojvodic, J. Kleis, P. Hyldgaard, and E. Schröder, New J. Phys. **12**, 013017 (2010).
[30]W. Wang, Y. Zhang, and Y.-B. Wang, J. Chem. Phys. **140**, 094302 (2014).
[31]R. Li, S. Hou, J. Zhang, Z. Qian, Z. Shen, and X. Zhao, J. Chem. Phys. **125**, 194113 (2006).
[32]See supplementary material at http://dx.doi.org/10.1063/1.4918738 for the atomic and electronic structures of the infinite one-dimensional polyacene, the atomic and electronic structures of N-doped graphene, the atomic structure and the electronic transport properties of the C6 alkyne chain connected directly to two semi-infinite N-doped graphene electrodes, the LDOS of the carbon atom at the zigzag edge of semi-infinite N-doped graphene electrodes, and effects of spin polarization at the zigzag edges on the junction transport properties.
[33]K. H. Khoo, J. B. Neaton, Y. W. Son, M. L. Cohen, and S. G. Louie, Nano Lett. **8**, 2900 (2008).
[34]G. P. Zhang, X. W. Fang, Y. X. Yao, C. Z. Wang, Z. J. Ding, and K. M. Ho, J. Phys.: Condens. Matter **23**, 025302 (2011).
[35]L. Shen, M. Zeng, S. Yang, C. Zhang, X. Wang, and Y. Feng, J. Am. Chem. Soc. **132**, 11481 (2010).
[36]Z. Zanolli, G. Onida, and J.-C. Charlier, ACS Nano **4**, 5174 (2010).
[37]B. Akdim and R. Pachter, ACS Nano **5**, 1769 (2011).
[38]T. Schiros, D. Nordlund, L. Pálová, D. Prezzi, L. Zhao, K. S. Kim, U. Wurstbauer, C. Gutiérrez, D. Delongchamp, C. Jaye, D. Fischer, H. Ogasawara, L. G. M. Petterson, D. R. Reichman, P. Kim, M. S. Hybertsen, and A. N. Pasupathy, Nano Lett. **12**, 4025 (2012).
[39]P. Moreno-García, M. Gulcur, D. Z. Manrique, T. Pope, W. Hong, V. Kaliginedi, C. Huang, A. S. Batsanov, M. R. Bryce, C. Lambert, and T. Wandlowski, J. Am. Chem. Soc. **135**, 12228 (2013).
[40]D. A. Ryndyk, J. Bundesmann, M.-H. Liu, and K. Richter, Phys. Rev. B **86**, 195425 (2012).
[41]J. A. Furst, M. Brandbyge, and A. P. Jauho, Europhys. Lett. **91**, 37002 (2010).
[42]K. A. Ritter and J. W. Lyding, Nat. Mater **8**, 235 (2009).
[43]L. Sun, P. Wei, J. Wei, S. Stefano, and S. Hou, J. Phys.: Condens. Matter **23**, 425301 (2011).
[44]R. Mondal, R. M. Adhikari, B. K. Shah, and D. C. Neckers, Org. Lett. **9**, 2505 (2007).
[45]S. Bailey, D. Visontai, C. J. Lambert, M. R. Bryce, H. Frampton, and D. Chappell, J. Chem. Phys. **140**, 054708 (2014).